Characteristics and origin of Microfracture in Lower Cretaceous Tight Sandstone from Kuqa Foreland Basin, NW China*

Chun Liu[1], Ronghu Zhang[1], Huiliang Zhang[1], Xianzhang Yang[2], and Junpeng Wang[1]

Search and Discovery Article #10514 (2013)
Posted August 26, 2013

*Adapted from extended abstract prepared in conjunction with poster presentation at AAPG Annual Convention and Exhibition, Pittsburgh, Pennsylvania, May 19-22, 2013,

[1]PetroChina Hangzhou Research Institute of Geology, Hangzhou, China (liuc_hz@petrochina.com.cn)
[2]PetroChina Tarim Oil Field Company, Korla, China

Abstract

The Kuqa basin, as a secondary tectonic unit of Tarim basin, located at the front of the south Tianshan Mountain, is a foreland basin formed in the Late Tertiary. The Lower Cretaceous Bashijiqike tight sandstone in the basin is an ultralow-permeability and low-porosity reservoir. Microfractures, such as intragranular microfractures, grain-edge microfractures, and transgranular microfractures, are abundant in the tight sandstones. Microfractures improve storage and permeability and impact distribution of natural gas. Microfractures have a wide range of sizes, shapes, and patterns, but most of them are opening-mode fractures. Microfractures reflect tectonic, overpressure, and diagenetic origins. Based on fluid inclusions, carbon-oxygen stable isotope analysis of fracture-filling cements (calcite and dolomite) and burial history, tectonic microfractures were determined to be formed before early Miocene and at the middle of Miocene. In the middle to late Himalayan movement, the tension microfractures closed and were filled with carbonate cements. Microfractures related to overpressure, being tension microfractures, are commonly filled with bitumen and were formed at the end of Miocene. The transition of stress state from compression to tension by overpressure is the reason that tension microfractures were formed in the compression setting. Diagenetic fractures were formed at the end of the Late Cretaceous to Paleogene. Under intense compaction, grain-crushing crackle fractures in quartz and cleavage fractures in feldspar formed intragranular microfractures. Some transgranular microfractures and grain-edge microfractures caused by diagenesis are along the bedding plane and parallel to the directional mineral grains.

Introduction

In siliciclastic hydrocarbon reservoir rocks, economic gas and oil production may depend on the attributes of natural fractures, and, with the advent of horizontal drilling, fractures are increasingly exploration and development targets (Stephen, 1997). Fractures are important fluid-flow conduits in the subsurface and important repositories of oil and gas. Analysis of core samples and imaging logging can provide the most direct method to evaluate large fractures (macrofractures) in the subsurface. However, natural microfracture properties are rarely known

in evaluation and reservoir development planning simply because most large fractures do not intersect well bores where they can be detected and characterized. The characterization of microfractured reservoirs continues to challenge geoscientists.

Microfractures are common features in most rocks and occur in a variety of forms (Kranz, 1983). Some microfractures are partly or completely closed with secondary minerals or are visible only as planes of fluid inclusions, whereas other microfractures are open, have sharp sides, and lack secondary minerals. In rock samples obtained from the subsurface by coring, the origin of nonmineralized microfractures is often uncertain. Such fractures can result from natural subsurface processes, drilling, core expansion or contraction during or shortly after coring, core handling, or sample preparation. In contrast to large fractures, microfractures are commonly more abundant in the same volume of rock (Ortega and Marrett, 2000; Ortega et al., 2006) and can provide in on the associated macroscopic fractures. Microfractures can also be used as paleostress indicators, strain gauges, and markers of de timing (Laubach, 1989). In sedimentary rocks, description of microfracture populations that have been fossilized by authigenic cements involves high-magnification measurement (Onasch, 1990; Laubach, 1997; Ortega and Marrett, 2000; Wilson et al., 2003). Ortega and Marrett (2000) reported prediction of macrofracture properties using microfracture in and found that systematic analysis of abundant microfractures in small pieces of rock could overcome the severe limitations of acquiring subsurface macrofracture data. Gomez and Laubach (2006) reported rapid digital imaging and quantification methods vital for analysis of microfracture populations. This approach can provide key evidence for numbers of sets, strike, crosscutting relations, strain, the volume of microfracture-sequestered cement, and meaningful data on microfracture population size and spacing patterns that would not be evident otherwise.

The Kuqa Basin was the important natural gas producing area in China. The largest commercial gas field, Kela 2, was found in 1998. Natural gas in the Kuqa basin is mainly distributed in the Lower Cretaceous Bashijiqike tight sandstone and controlled by structures and fractures. The Lower Cretaceous Bashijiqike tight sandstone is an important natural gas play in the Kuqa foreland basin. Microfractures are well developed in the tight sandstone. At present, commercial gas flows have been found in several structures, including Dabei, Kela, and Dina. The tight sandstone has great potential as a natural gas resource, and it is becoming a significant exploration target in the Tarim basin (Zhang Lijuan, et al., 2006). Recent research indicates that microfractures in these rocks provide important storage space and increase the permeability of these tight sandstones (Liu Chun et al., 2009). Microfractures are likely a key factor for controlling natural gas accumulation and high production rates (Zhang Ronghu et al., 2008ab, 2010; Zhang Huiliang et al., 2012). Therefore, understanding the characteristics and origin of microfractures has great significance for natural gas exploration and development in Kuqa foreland basin.

Some scholars have studied fractures in the Lower Cretaceous Bashijiqike tight sandstone of the Kuqa Basin. Zeng Lianbo (2004) discussed the distribution of fractures in typical structures of Kuqa Basin. They divided fractures into northwest-southeast, northeast-southwest and approximate north-south tectonic fractures with medium-high dip angles in the depression. Zhang Fuxiang et al. (2006) emphasized the contribution of fractures of Kuqa foreland fractured sandstone gas reservoirs to permeability. Zhang Bo et al (2011) also analyzed the differences in fracture intensity correlate with rock properties, such as rock type, bed thickness, microfacies, porosity, and presence of microlayering. Liu Chun et al. (2009, 2010) used the relationship of fractures with mineral grains to divide microfractures into three types: intragranular microfractures, grain-edge microfractures, and transgranular microfractures.

Core and cast sections observation and description, and imaging logging, scanning electron microscope and core lab analysis data etc. were applied to present the characteristics a and origin of microfractures in the Lower Cretaceous Bashijiqike tight sandstone in the Kuqa foreland basin. In this article, 334 conventional thin sections from 17 wells, 175 casting thin sections injected with epoxy from 12 wells, and 67 scanning electron microscope samples from 9 wells, 5 carbon-oxygen stable isotope analysis of fracture-filling cements (calcite and dolomite) from 2 wells. Samples are from the Dabei, Keshen, and Kuche River field outcrop structures of the Lower Cretaceous Bashijiqike tight sandstone in the Kuqa foreland basin.

Geologic Setting

Structure. The Kuqa foreland basin, bounded to the north by the South Tianshan Mountains, is a secondary structural unit within the northern Tarim Basin (Figure 1). This foreland basin formed since the Late Tertiary (Tian Zuoji et al., 1999).One main group of northeast-southwest and its associated fold structures exist. The faults have high throw and have trace lengths of tens of kilometers. Most faults cut the whole Triassic to the Lower Eogene strata, but several cut Cenozoic strata (Figure 2).

Stratigraphy and Sedimentology. Before the late Jurassic, the Kuqa Basin was dominated by lacustrine-swamp deposition. From the Late Jurassic, the depression was filled with continental detrital deposits with a gross thickness of more than 2,000m (6,562 ft), and is typical continental sedimentation system. The Lower Cretaceous Bashijiqike tight sandstone, the primary gas-bearing unit and the primary exploration target in Kuqa foreland basin, can be subdivided into K_1bs^3, K_1bs^2 and K_1bs^1 from bottom to top (Figure 3).

Facies include alluvial fan, river, lake, and delta. The basal K_1bs^3 interval comprises fan delta plain conglomerate or pebbled medium-grain sandstone, fan delta fine-grain sandstone or siltstone and pro-delta mudstone (Jia Jinghua et al., 2000; Zhang Lijuan et al., 2006).The K_1bs^2 is overlain directly by the K_1bs^3, which mainly consists of braided delta front and braided delta plain, and is made of conglomeratic sand, medium-fine grain sandstone and siltstone. The total sandstone proportion from 60%-80%,the maximum can be up to 95 %.Most of these sandstones are composed of feldspathic, lithic feldspathic and lithic sandstone with 30 %～50 % of quartz and rich in lithoclast. Sedimentary structures are mainly massive bedding, large t rough cross bedding and oblique bedding with few parallel bedding, wave bedding and horizontal bedding. Main sedimentary period of the braided channel is flood stage, so the sedimentation is characterized by rapid migration of channels with different stages to form thick and continuous sandstone layers by lot s of super imposed sand bodies, which are separated by some thin intercalated pelitic beds (Gu Jiayu et al., 2001). The overlying K_1bs^1 consists of braided delta plain facies. The thickness is very thin, and the distribution range is very limitation due to erosion. Therefore, the K_1bs^2 is of vital importance for gas production.

Reservoir Characteristics. The deltaic sandstone of the first member of the Bashijiqike tight sandstone is the principal gas reservoir in Kuqa foreland basin; other members are the secondary gas reservoir (Liu Chun et al., 2009). The thickness of sandstone is more than 70% of that of the gross stratum. In addition, the burial depth is more than 6,000 m (19,686 ft), whereas the reservoir thickness is 100 to 200 m (328–654 ft). The physical properties of the tight sandstone reservoir are obtained from core analysis. The Bashijiqike tight sandstone is fine- to coarse-grained; grains are sub-angular to subrounded with moderately sorted. Minor clay matrix (pseudomatrix and epimatrix). Derived from mechanical and alteration of the metamorphic rock fragments, and feldspars, occurs in all sandstone samples (< 1%). Quartz grains are

monocrystalline with frequent corrosion cavities (pits). Few polycrystalline grains are present. Rock fragments are volcanic, metamorphic (quartzite) and sedimentary (< 2%). Minor heavy minerals are present. According to an analysis of 300 rock samples from the Dabei, Keshen structures, the Bashijiqike tight sandstone are tough and compact, and average porosity of core plugs from 156 samples is 3.57%, with a range from 0.65 to 7.24 % (Figure 4A). These values match well with two-dimensional estimates from thin sections, which average 2.7%. A few porosity estimates from thin sections were as high as 11.6% and inspection shows that these more porous samples are either highly fractured or contain an unusual abundance of partially dissolved feldspar. Permeability of the 151 samples averages 0.359mD, with a maximum value of 33.7mD (Figure 4B). These porosity and permeability values are very low, which correlation is very poor (Figure 5). Therefore, the Bashijiqike sandstone is a typical tight reservoir of low porosity and ultralow permeability.

The reservoirs can be classified as fractured in that they produce despite having low porosity, small pores, complicated pore configurations, poor connectedness, high water saturation - normally 60 to 70% - and strong anisotropy. Microfractures are the main factors improving the storage as well as the permeability of the tight sandstones. The contribution is 99.08% of the total permeability in tight sandstones of Dabei gas field (Zhang Fuxiang, 2011). The average sandstone intragranular and intergranular porosities are only 0.5-3%. The average permeabilities caused by microfractures are 0.36 mD. Using core analysis data, the relationship between permeability and porosity is shown in Figure 5. When samples have no microfractures, the permeabilities of samples are less than 0.1 mD. Several samples have microfractures, and their permeabilities can exceed 1 mD. The fractures have an obvious sensitivity to stress (Smart et al., 2001; Zeng et al., 2007c). As the scale and permeability of the fracture increase, the stress sensitivity increases (Zeng and Li, 2009), so fracture porosity and permeability at reservoir condition will be lower than that at surface conditions. The existence of overpressure in the tight-gas sandstones and partial filling in some microfractures will greatly weaken the change in microfracture porosity and permeability caused by subsurface conditions in the Kuqa Basin.

Microfracture Types and Characteristics

Microfracture types. Microfracture and macrofracture characteristics and abundance were determined in core specimens from one s consisting of two gas reservoirs. About 400 thin sections were examined for expression of microfractures using optical microscopy or scanning electron microscope. Sample geology is summarized in Table 1. Specimens used in this study are mainly fine- to medium-grained rock-fragment sandstone with variable cement volume and are from depths ranging from 5,000 to 7,000 m. Subvertical opening-mode macrofractures that are filled or lined with carbonate, and locally with other minerals, are visible in cores and field outcrop from all of the tight sandstone(Figure 6). The units were chosen for study because their fractures are inferred to be important to production. Microfractures have a wide range of sizes, shapes, and patterns, but most of them are opening-mode fractures (i.e., formed by opening movement normal to fracture walls). They can be divided into three categories based on the relation of fractures to grains: intragranular microfractures, grain-edge microfractures, and transgranular microfractures (Table 2).

Category I. Intragranular microfractures, lying entirely within grains, are mainly irregular arrays within quartz and cleavage fractures in feldspar. Microfractures having curved to straight traces arranged in simple to complex intersecting patterns. They are developed within quartz or feldspar grains and typically are found where grains contact one another. They do not cut through the edge of mineral grains (Figure 7). Intragranular microfractures have apertures less than 10 μm and lengths equal to or smaller than grain size but locally have high

densities (Figure 7B). In some cases, crushed grains are associated with microbreccia along grain contacts and locally within cement. Such features in other sandstones were described by Milliken (1994). Textural relations indicate that these fractures formed mainly before or during early stages of quartz cementation, consistent with local large displacements and rotations of grain fragments within (now cement-filled) pore space.

Category II. Grain-edge microfractures are associated and may be coincident with the grain boundary. They are mainly distributed at boundaries between mineral grains along linear contacts (Figure 8), so that they can also be called intergranular microfractures. Grain-edge microfractures are narrow and short, with the apertures less than 10μm (Figure 8), although they have experienced dissolution, a few are as large as 20μm. The intragranular and grain-edge microfractures are not only important storage space of natural gas, but also are channels that link tiny pores and increase connectivity in otherwise ultralow-permeability reservoir rocks.

Category III. In contrast with grain-scale microfractures, the transgranular (traversing grain) microfractures are wider and longer. Length is not restricted by the size of mineral grains. They include fractures having generally straight traces in plan view and cross section, which indicates that they are planar. These fractures cut grain boundaries and cements without having any consistent relation to grain centers or grain contacts (Figure 9A, B). Displaced grain boundaries demonstrate that fracture opening was by dilation normal to fracture walls. The largest are transgranular fractures that cross several to tens of grains and intervening cement. In several samples from various depths, this category includes fractures that have crack-seal microstructure and crystal growth morphology identical to that of nearby macrofractures; texturally, these fractures are smaller versions of the large fractures. Shorter fractures that extend across single grains and adjacent cement, as well as minute fractures that are localized within cement or grains, have a similar appearance.

Transgranular fractures are lens shaped and gradually taper to sharp terminations in both plan view and cross section (Figure 9). In some cases, fractures end at grain–cement boundaries or subdivide into multiple strands near such contacts; however, fractures more commonly cross such boundaries with no def lection, implying that only slight mechanical contrasts existed between quartz grains and quartz cement during fracture growth. These patterns show that most fractures in this category grew after most of the quartz cement had been emplaced in these rocks. De occurred after sand became moderately to strongly indurated as a result of quartz cementation, so that it had low porosity and displayed homogeneous rather than aggregate behavior.

Microfractures having lengths greater than 100 μm are typically less than 10 μm wide, because narrow fractures with long traces are easy to identify, fractures with widths of less than 0.5 μm can be detected regularly at magnifications of 200 to 500. Their apertures are generally less than 40 μm, with peak values of 10 to 20 μm, but they may be more than 40 μm after being widened by dissolution. Fractures are either isolated or in subparallel groups. In a few instances, relay or en echelon patterns and parallel to anastomosing, intersecting swarms are evident. Although locally fractures concentrate within a few millimeters of large fractures or stylolites, other samples having high microfracture concentrations are not located near visible structures.

According to analysis of thin sections from 10 wells, almost all contain intragranular microfractures and grain-edge microfractures. Intragranular microfractures and grain-edge microfractures have high densities but small scales. Their effects on permeability can be expected to be small, but because of their abundance, they are the main microfracture storage in these reservoirs. Porosity associated with these fractures

is comparable in magnitude to that of the matrix pore system. Thin sections with transgranular microfractures are less common, comprising only 16% of all thin sections. The density of transgranular microfractures is higher around faults and on the high parts of structures.

Microfracture Origin

Tectonic origin. With intense tectonic compaction, sandstone becomes densified and fractures occur, resulting in fractured reservoirs with high production (Li Jun et al., 2011). Among the three types of microfractures, most of the transgranular microfractures are tectonic. These tectonic microfractures are present in most sandstone rock types. They are partly filled with calcite or anhydrite. The tectonic microfractures are long, have a regular distribution, and are part of the same macrofracture populations that are associated with folds and thrusts. In addition, some intragranular microfractures are also related to tectonic compression.

The timing of fractures was deduced from fluid inclusion of quartz and calcite deposits in the tectonic microfractures (Liu Chun et al., 2009). Raman microprobe spectrometer analysis shows that fluid inclusions are trapped during anhydrite and calcite-cement precipitation, mostly in the microfractures. Fluid inclusions, distributed as a string of beads or an oriented group, may be rectangular, irregular, or triangular. Typical inclusions in samples are smaller than 0.1 mm. Many are vapor and liquid, and their proportion ranges from 5 to 8%. Using methods outlined by Roedder (1984), we measured fluid-inclusion homogenization temperatures in 84 samples collected from the DB-KS gas field (Figure 1). Fluid-inclusion assemblages in 57 samples have homogenization temperatures that range from 100 to 142°C in KS gas field, average 129°C. These homogenization values are close to the values of 97 to 157.8°C in 27 samples collected from the DB gas field, average 120°C.

According to overlapping relations of minerals in micro-fractures, their fluid inclusion analysis, and carbon-oxygen stable isotope analysis of macro-fracture-filling cements (calcite and anhydrite), I deduce the tectonic have two tectonic events and one crack-filling event, which showing that tectonic microfractures mainly formed in the second tectonic events, fracture-filling cements (calcite and anhydrite) event was the first tectonic event. The first tectonic event was before early Miocene (about 18Ma) based on oxygen stable isotope analysis of fracture-filling cements with carbonate cement equilibration temperature range approximately 91 to 99°C (Table 3, Figure 10). The continuous tectonic event was middle Miocene (about 12 Ma) based on the fluid-inclusion in quartz boundary of microfracture with fluid-inclusion homogenization temperatures approximately from 100 to 150°C. For this reason, we deduce the Miocene was a crucial formation time of tectonic fracture, in which fracture (micro and macro) was formed and partly filled. The macro-fracture that can be seen in core takes place since early Pleistocene because of tectonic compression of South Tianshan.

Overpressure origin. I interpret some microfractures to be the result of overpressure because they are associated with veins filled with bitumen, and they may contain bitumen themselves. A bitumen-filled microfracture generally is wide and short. Based on the geometry of these bitumen-filled microfractures, they are tensional veins, which are the products of tension stress, and the veins are perpendicular to the minimum principal stress direction. It is suggested that the tectonic compression is one of the main factors resulted in the incremental pore fluid pressure of Mesozoic reservoirs in northern Kuqa depression. The tensile stress effect formed by South Tianshan tectonic movement and the developed salt rock in the key strata are two important factors for forming such an overpressure in Kuqa basin (Tang Shaobao et al., 2011).

According to the analysis of mechanism of overpressure, burial history, and hydrocarbon generating in the Kuqa foreland basin, the overpressure began to form at the end of the early Pleistocene (Zeng Lianbo, et al., 2006). The overpressure resulted in many microfractures (Zha Ming et al., 2000). Cenozoic tectonic movements at the south of the Kuqa basin were intense, and the overpressures were released with fault activity and uplift as seals were breached. When pore-fluid pressure dropped to 60% of static pressure in the upper strata, the overpressure-related microfractures would close or could be filled with calcite (Zeng Lianbo, 2010). According to fluid-inclusion analysis from the DB gas field, the homogenization temperatures of these calcite veins are 90 to 110°C, combined with paleogeothermal gradients and burial history analysis, the filling period result from overpressure for calcite veins was early Miocene (Figure 10).

Diagenetic origin. Microfractures are defined as diagenetic features that formed during physical diagenesis. Diagenetic fractures can be transgranular microfractures, intragranular microfractures, and grain-edge microfractures. Transgranular microfractures formed during diagenesis are mainly present on the boundaries between sandstone and mudstone, parallel to the directional compaction fabric of platy minerals (and thus parallel to bedding). They are especially well developed in argillaceous rocks (Figure 11). This type of diagenetic fracture commonly develops along microlayers, where layers bend, end, pinch, or branch; they are commonly filled with clay minerals. The intragranular microfractures and grain-edge microfractures are diagenetic fractures because they were formed during compaction. Grain-edge microfractures commonly occur together with intragranular microfractures. The more compacted the rock, the less debris is present in the rock; the rougher the grains that contact each other in a linear manner, the better the intragranular fractures and grain boundary fractures will be developed. The sandstone of intragranular fractures is mainly related to intensive mechanical compaction. The sandstone of grain-edge microfractures is associated with intensive compaction and pressure solution. According to diagenetic analysis, the formation time of these diagenetic microfractures was mainly from the early Paleocene to early Miocene (Liu Chun et al., 2009).

Discussion

Microfractures are commonly filled with anhydrite, calcite, bitumen, and clay minerals. Clay commonly fills in diagenetic microfractures, bitumen is in overpressure-related microfractures, and anhydrite and calcite are in tectonic microfractures. Two crack-filling events in tectonic microfractures indicate that they were formed in two tectonic movements. Therefore, the microfracturing sequences in the Lower Cretaceous Bashijiqike tight sandstone of the Kuqa basin can be divided as follows. First, the diagenetic microfractures were formed under intensive diagenesis and were filled with clay minerals. Diagenesis analysis suggests that the formation time of diagenetic microfractures was from the early Paleocene to early Miocene. Second, the tectonic microfractures formed in the early Miocene, and they commonly filled with anhydrite and calcite deposits. Then, at the end of middle Miocene, tectonic microfractures formed again because of compression and high fluid pressures. Third, with strata reaching the greatest burial depth and generating overpressure in the late Miocene, overpressures caused tensional microfractures filled with bitumen to form. Finally, Tectonic microfractures formed under intensive tectonic compression since early Pleistocene.

Tectonic microfractures are well developed in all of the gas fields and are the principal type in the Lower Cretaceous Bashijiqike tight sandstones in Kuqa foreland basin. The intensity of tectonic microfracture is controlled by structure and lithology. The tectonic microfracture is better developed in the hanging wall of thrusts and fine-grained sandstone. Diagenetic microfractures are asymmetrically developed in

different structures and are relative to debris content and compaction. The intragranular and grain-boundary fractures have wide-ranging distribution but small extent and size similar to that of the matrix pores and are a factor in storage of gas. Diagenetic microfractures distributed along the microbedding plane are discontinuous and closed under peripheral pressure, and so contribute little to production. Microfractures related to overpressure are short, have poor connectivity, are usually filled with bitumen and calcite, and so contribute little to production despite big apertures.

Conclusions

Three important types of microfractures, intragranular, grain-edge, and transgranular microfractures, developed in the Bashijiqike tight sandstones of the Kuqa basin. Microfracture reflects tectonism, overpressure, and diagenetic processes (compaction and pressure solution).

Tectonic micro-fractures formed during two periods. The first was under the influence of northeast to southwest shortening that accompanied formation of the Kuqa foreland basin before early Miocene. The second was during resumed folding and thrusting since late Pliocene.

The existence of overpressure reduced effective stress, promoting opening-mode fracture growth. Because of overpressure, the stress state can be altered from compression to tension in the fold-thrust belt, and tension fractures can form in a compressional tectonic setting. The existence of tension fractures can also be used as an indicator of ancient overpressure in a sedimentary basin.

Under rapid sedimentation and intense compaction, intragranular microfractures formed because of the crushing of quartz grains and cleavage in feldspar. At the same time, under the influence of compaction and pressure solution, diagenetic transgranular microfractures formed along the microbedding planes and are parallel to the directional fabric of platy minerals.

The intragranular and grain-boundary fractures are developed discretely at different structures, have small size and permeability, and are a major factor in storage of gas. Tectonic microfractures controlled by fold thrust and lithology are developed at all of the gas fields and have the largest contribution to gas production. Diagenetic microfractures distributed along the microbedding plane and microfractures related to overpressure have little contribution to gas production.

Acknowledgements

The author thanks Zhibin Huang, Bo Zhang, the senior engineers at the Tarim Field Branch, PetroChina Company Limited, for their constructive help. The author is particularly grateful to SE. Jiang Yiming for helping relevant experiment and Bo Wang for constructive comments on an earlier version of this manuscript. This study is financially supported by the National Key Science & Technology Foundation of China (No. 2011ZX05003-004).

References Cited

Gomez, L.A., and S.E. Laubach, 2006, Rapid digital quantification of microfracture populations: Journal of Structural Geology, v. 28, p. 883-894.

Gu, J., F. Hui, J-H. Jia, 2001, Diagenesis and Reservoir Characteristics of Cretaceous Braided Delta Sandbody in Kuqa Depression, Tarim Basin: Acta Sedimentologica Sinica, v. 19/4, p. 517-523.

Jia, J-H., 2000, Deposition sequence and reservoir of Cretaceous Bashijiqike in Kuqa foreland basin: Earth Science Frontiers, v. 7/3, p.331-341.

Kranz, R.L., 1983, Microcracks in rock: A review: Tectonophysics, v. 100, p. 449-480.

Laubach, S.E., 1989, Paleostress directions from the preferred orientation of closed microfractures (fluid-inclusion planes) in sandstone, East Texas Basin, USA: Journal of Structural Geology, v. 11, p. 603-611.

Laubach, S.E., 1997, A Method to Detect Natural Fracture Strike in Sandstone. AAPG Bulletin, v. 81/4, p. 604-623.

Li, J., C. Zhang, and J. Li, 2011, Tectonic compaction and its influence on reservoirs in the Kuqa foreland basin, Tarim: Petroleum Exploration and Development, v. 38/1, p. 47-51.

Liu, C., H. Zhang, and H. Bo, 2009, Reservoir characteristics and control factors of deep burial clastic rocks in Dabei zone of Kuqa Sag: Natural Gas Geoscience, v. 20/4, p. 504-512.

Liu, C., H-L. Zhang, and R-H. Zhang, 2010, Geochemistry Characteristic and Origin of Paleogene Dolomite in Kuqa Depression, Tarim Basin: Acta Sedimentologica Sinica, v. 28/3, p. 518-524.

Milliken, K.L., 1994, The widespread occurrence of healed microfractures in siliciclastic rocks: evidence from scanned cathodoluminescence imaging, *in* P.P. Nelson and S.E. Laubach, (eds.), Rock mechanics: models and measurements, challenges from industry: Rotterdam, A. A. Balkema, p. 825-832.

Ortega, O.J., and R.A. Marrett, 2000, Prediction of macrofracture properties using microfracture in, Mesaverde Group sandstones, San Juan Basin, New Mexico: Journal of Structural Geology, v. 22, p. 571-588.

Ortega, O.J., R.A. Marrett, and S.E. Laubach, 2006, A scale independent approach to fracture intensity and average spacing measurement: AAPG Bulletin, v. 90/2, p. 193-208.

Roedder, E., 1984, Fluid inclusions: Reviews in mineralogy: Mineralogical Society of American, v. 12, p. 644.

Tian, Z., 1999, Tertiary Structure Characteristics and Evolution of Kuqa Foreland Basin: Acta Petrolei Sinica, v. 20/4, p.7-13.

Tang, S-B., F. Gao, and H-H. Fan, 2011, Mechanism of Cretaceous-Paleogene Abnormal Pressure in Dabei Area of Kuqa Depression, Tarim Basin: Xinjiang Petroleum Geology, v. 32/4, p.370-372.

Wang, F., A. Du, Q. Li, 2005, Organic maturity and hydrocarbon generation history of the Mesozoic oil-prone source rocks in Kuqa depression, Tarim Basin: Geochimica, v. 34/2, p. 136-146.

Wilson, J.E., J.S. Chester, and F.M. Chester, 2003, Microfracture analysis of fault growth and wear processes, Punchbowl Fault, San Andreas system, California: Journal of Structural Geology, v. 25, p. 1855-1873.

Zeng, L.B., C.X. Tan, and M.L. Zhang, 2004, Tectonic stress field and its effect on hydrocarbon migration and accumulation in Mesozoic and Cenozoic in Kuqa depression, Tarim Basin: Science in China Series D-Earth Sciences, v. 47, supplement 2, p. 114-124.

Zeng, L., and T. Zhou, 2004, Reservoir Fracture Distribution law of Kuqa depression in Tarim basin: Natural Gas Industry, v. 24/9, p.23-25.

Zeng, L.B., and B.M. Liu, 2006, Overpressure in Kuqa foreland thrust zone, Tarim Basin, NW China: Origin and its impacts on hydrocarbon accumulation: Progress in Natural Science, v. 16, p. 1307-1314.

Zeng, L.B., J.F. Qi, and Y.X. Wang, 2007d, Origin type of tectonic fractures and geological conditions in the low permeability reservoirs (in Chinese with English abstract): Acta Petrolei Sinica, v. 28/4, p. 52-56.

Zeng, L., Z. Wang, S. Xiao, 2009, The origin and geological significance of low dip-angle fractures in the thrust zones of the western basins of China: Acta Petrolei Sinica, v. 30/1, p.56-60.

Zeng, L.B., and X.Y. Li, 2009, Fractures in sandstone reservoirs of ultra-low permeability: The Upper TriassicYanchang in the Ordos Basin, China: AAPG Bulletin, v. 93/4, pp. 461-477.

Zha, M., 2000, The character and origin of overpressure and its exploration significance in Junggar basin: Petroleum Exploration and Development, v. 27/2, p.31-35.

Zhang, L-J., D-L. Li, and Y-S. Sun, 2006, Analysis of characteristics of sedimentary reservoir between Cretaceous and Palaeogene in the western part of the Kuqa depression: Natural Gas Geosciences, v. 17/3, p. 355-360.

Zhang, R., H. Zhang, and Y. Ma, 2008, Origin of extra Low porosity and permeability high production reservoirs: A case from bashijiqike reservoir of Dabei 1 oil field, Kuqa depression: Natural Gas Geosciences, v. 19/1, p. 75-82.

Zhang, R., H. Zhang, and J. Shou, 2008, Geological analysis on reservoir mechanism of the lower cretaceous Bashijiqike in Dabei area of the Kuqa depression: Chinese Journal of Geology, v. 43/3, p. 507-517.

Zhang, F. X. Wang, and Y. Li, 2011, The contribution of Fractures of Kuqa foreland Fractured Sandstone Gas Reservoirs to Permeability: Journal of Oil and Gas Technology, v. 33/6, p.149-152.

Zhang, B., W. Yuan, and S. Cao, 2011, Fuzzy-synthetical Evaluation of Main Factors of Fracture in Dabei Gas Field: Natural Gas Geoscience, v. 22/2, p.250-253.

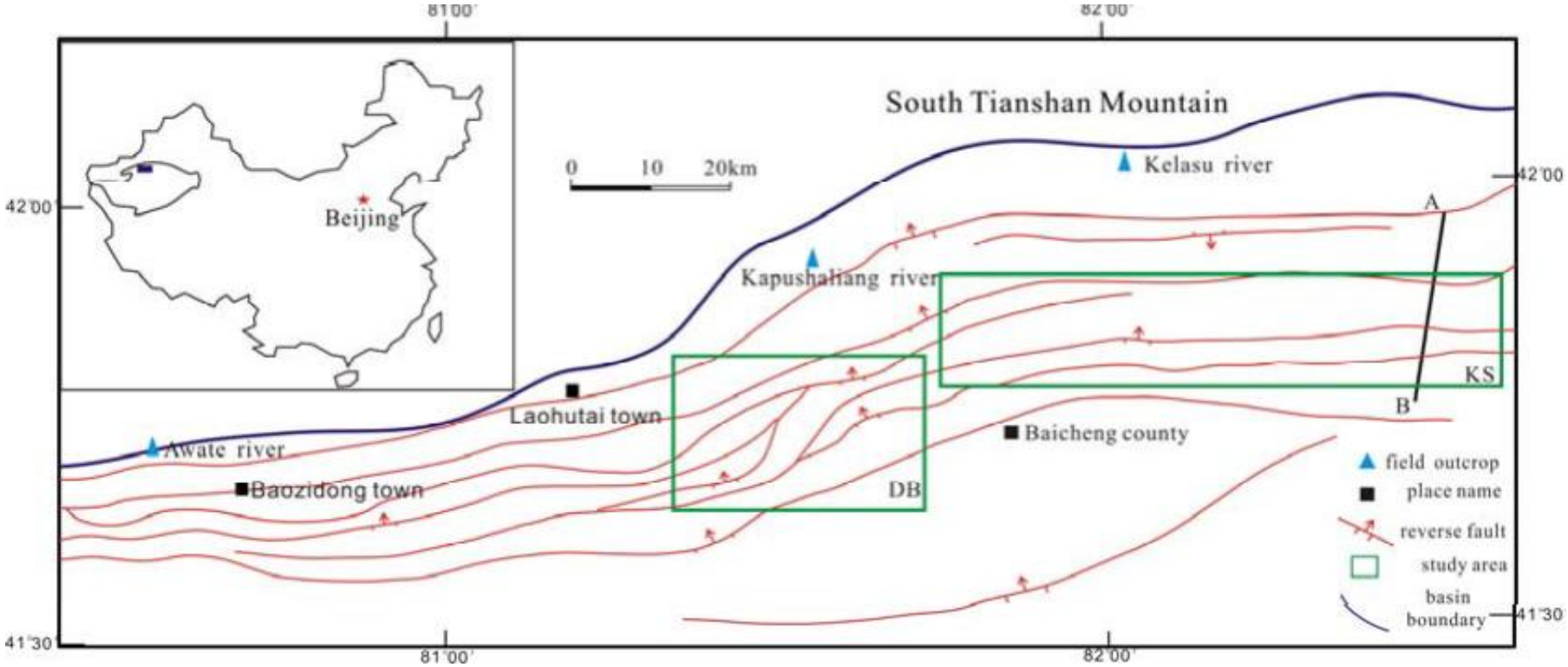

Figure 1. Map showing location of the South Tianshan Mountain fold-thrust belt, Kuqa foreland Basin, and study area (green small box). Red lines are reverse faults. Bar indicates dip and arrow marks slip direction. DB=Dabei gas field; KS=Keshen gas field.

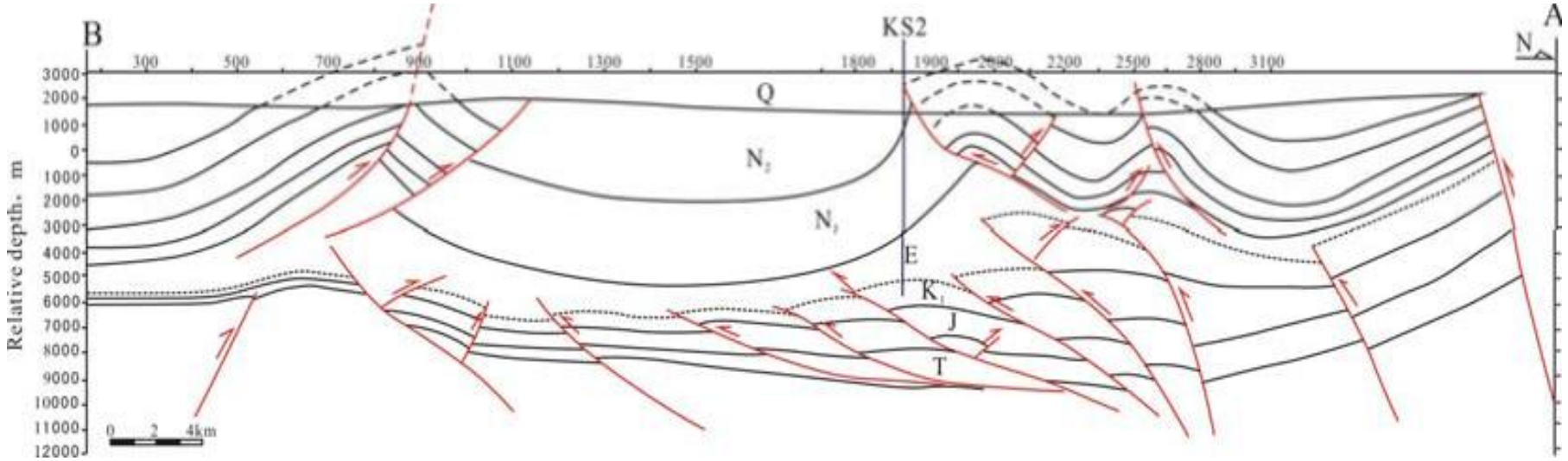

Figure 2. Structural cross section based on surface geology and seismic data. Line location is shown in Figure 1. KS2 is a well.

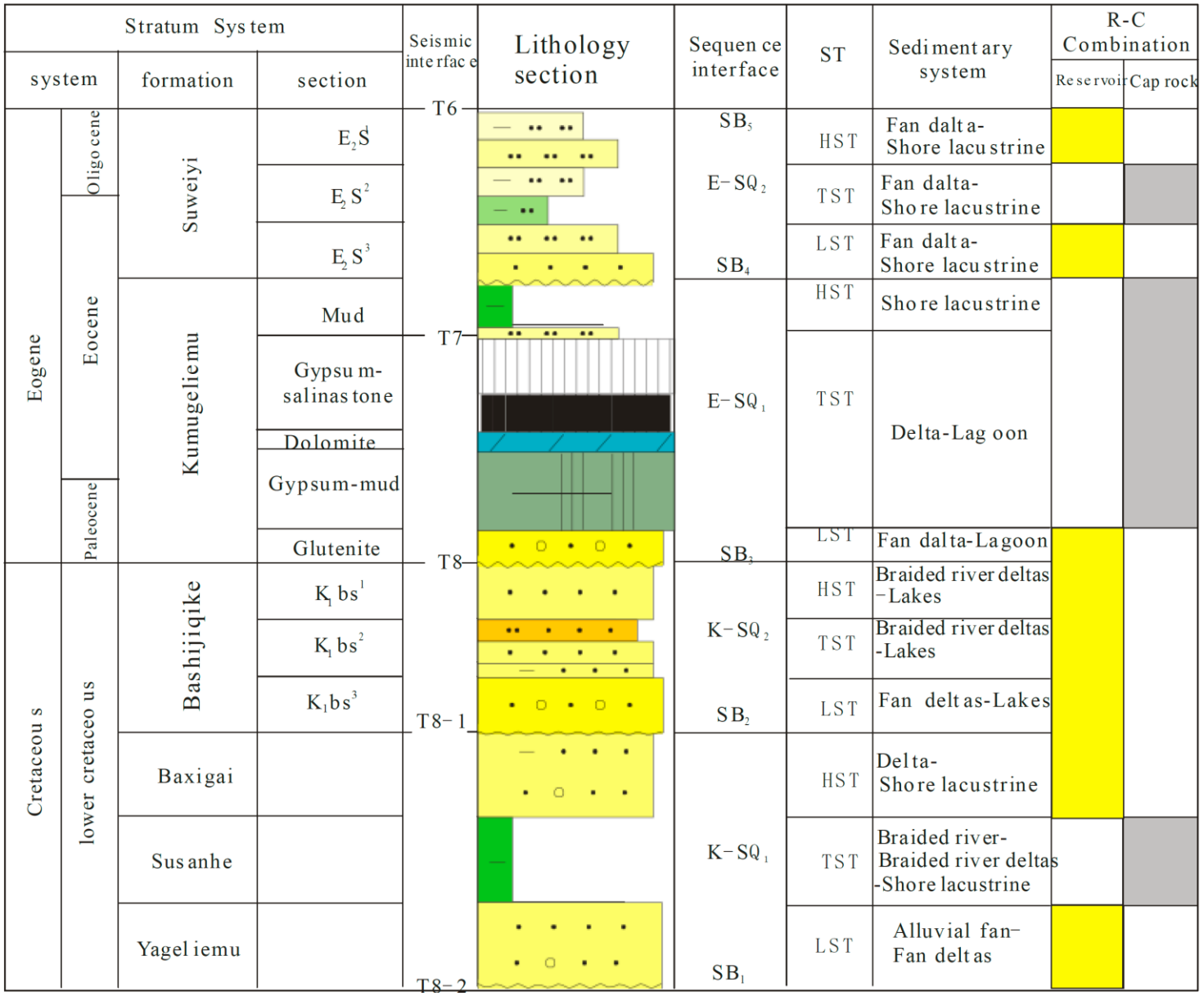

Figure 3. Simplified Lower Cretaceous to Eogene stratigraphy of Kuqa foreland basin.

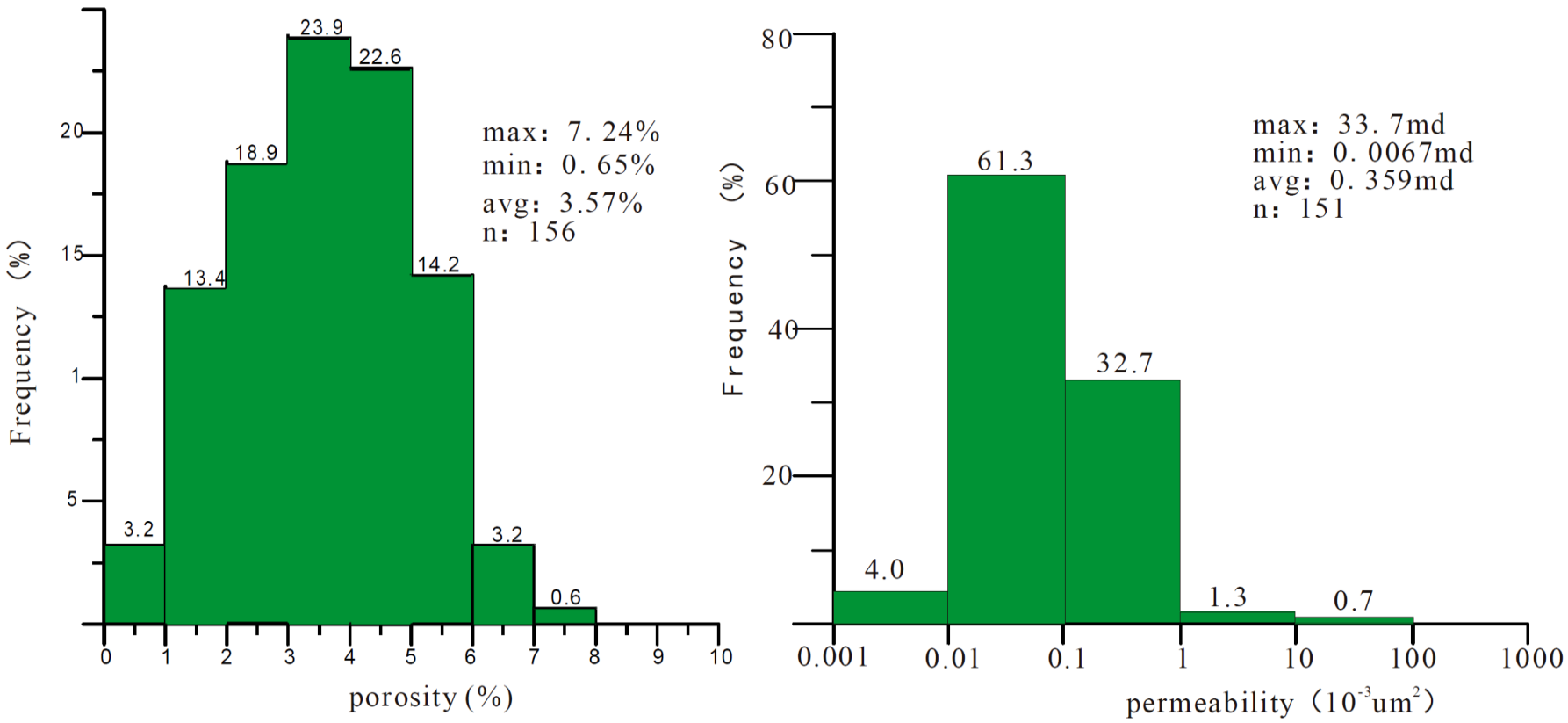

Figure 4. Frequency plots of A) porosity and B) permeability distributions.

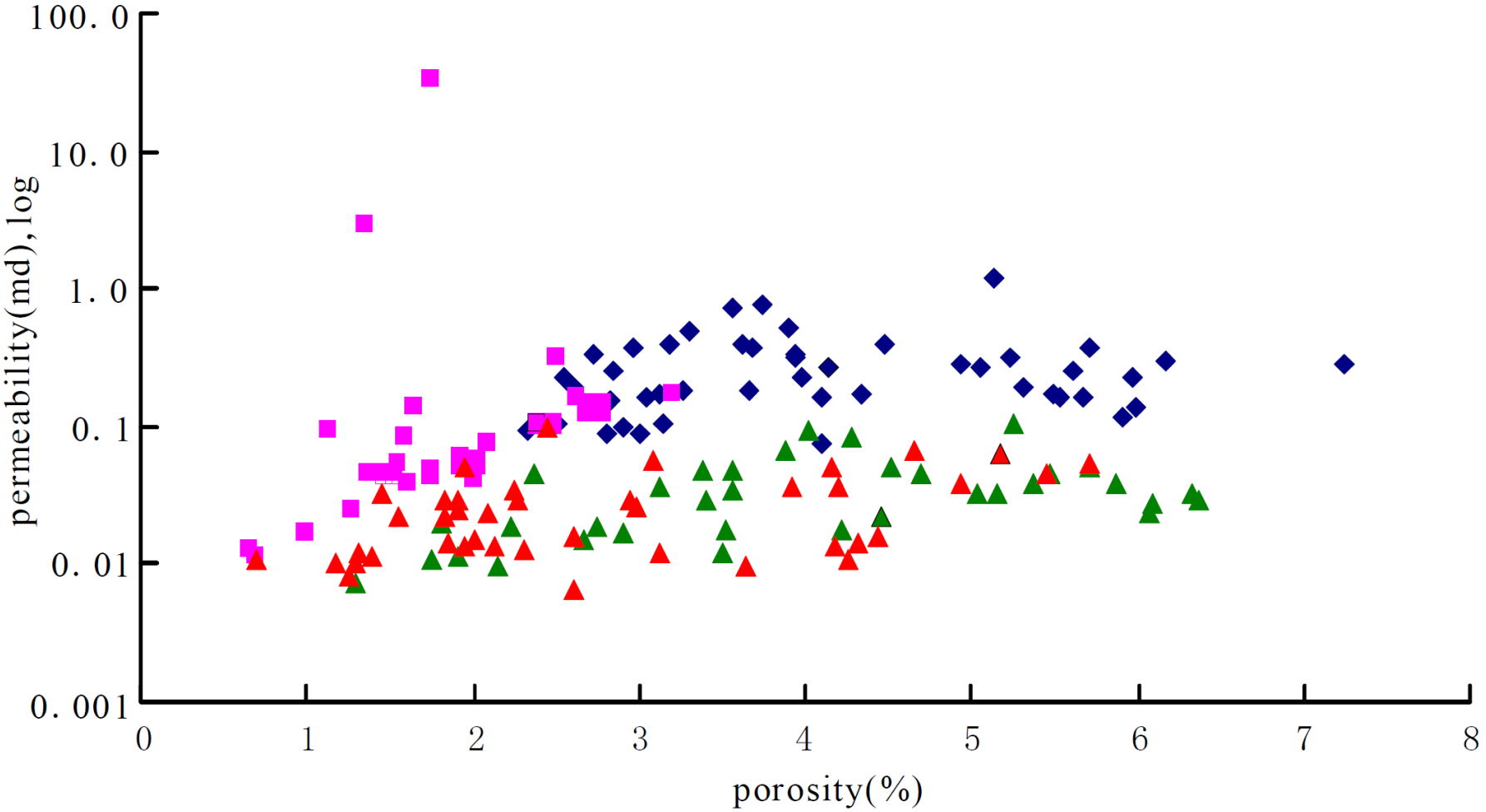

Figure 5. Relationship between the permeability and porosity from 156 core samples in the Lower Cretaceous Bashijiqike tight sandstone, Dabei-Keshen gas field, Kuqa foreland basin.

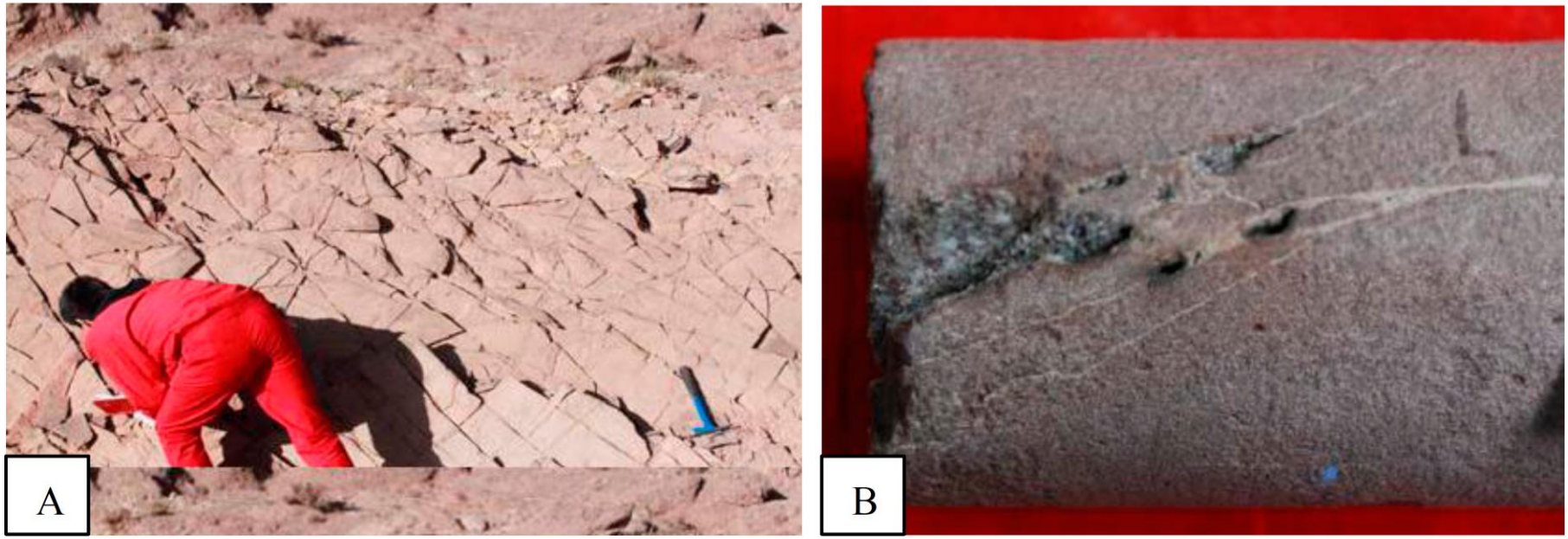

Figure 6. The characteristics of macrofracture in the Lower Cretaceous Bashijiqike tight sandstones. A=the field outcrop of Kuche River; B: the core of KS201 well.

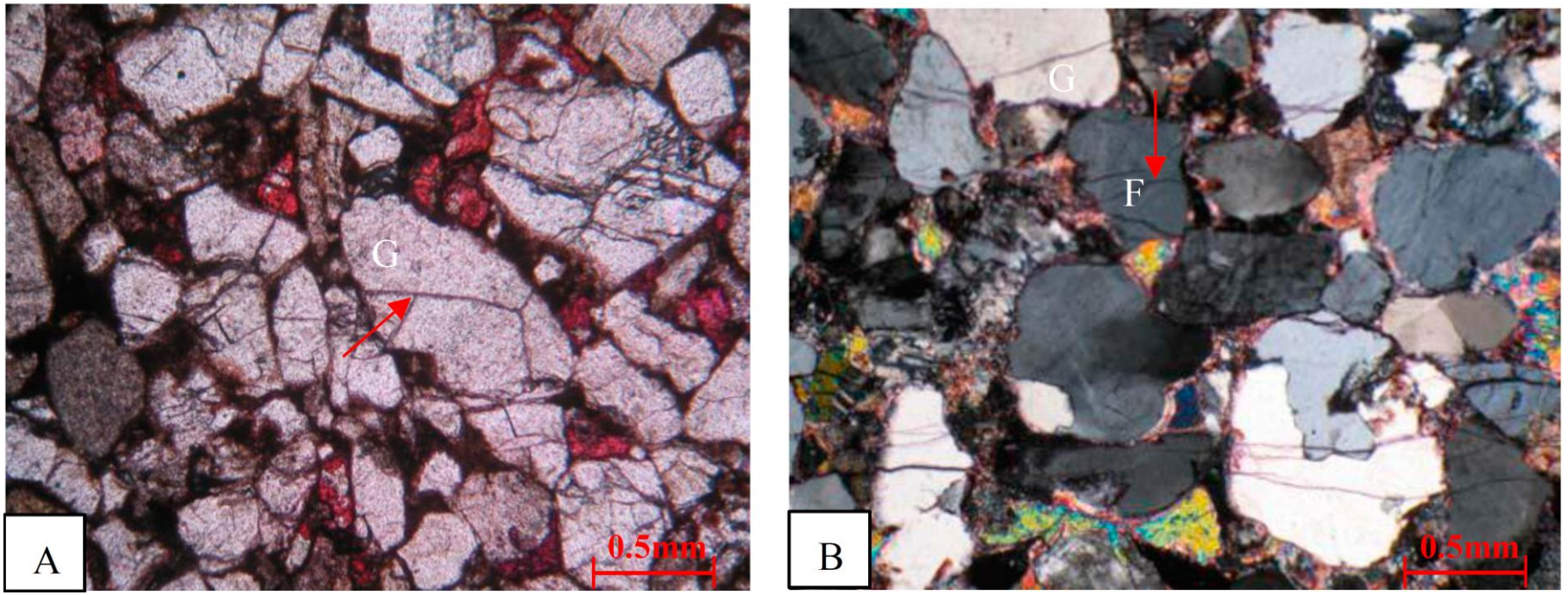

Figure 7. Intragranular microfractures (arrow) in thin section. A=intragranular microfracture formed within a crushed quartz grain from KS gas field, depth 6,780m (22,245ft). Plane-polarized light, PPL; B = intragranular microfracture formed within a crushed quartz and feldspar grain from KS gas field, depth 5,685m (18,652.5ft). Crossed polarizers light, XPL.

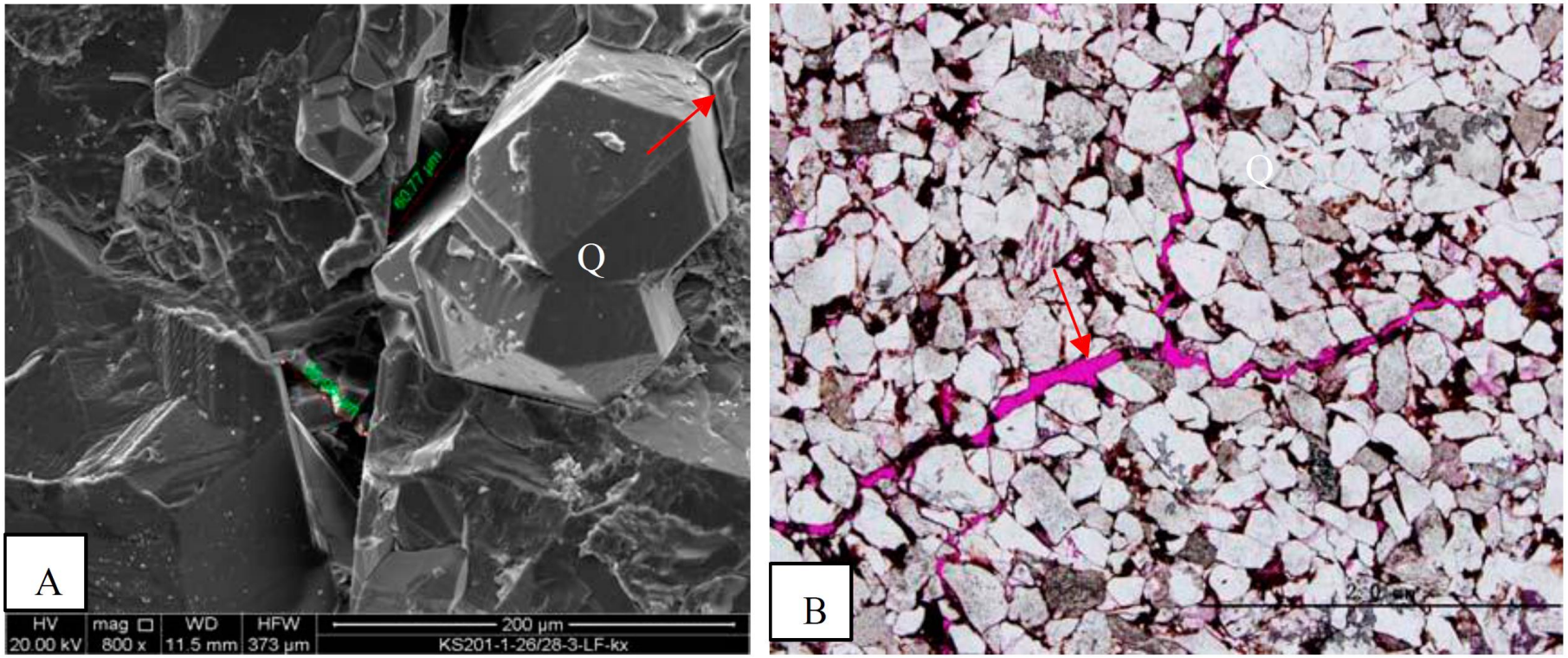

Figure 8. Grain-edge microfracture (arrow) along boundary of quartz grain from KS gas field, A=specimen from depth of 6,706m (22,002ft).Scanning electron microscope (SEM); B= specimen from depth of 6,669m (21,881ft), Plane-polarized light, PPL. Red is the epoxy resin.

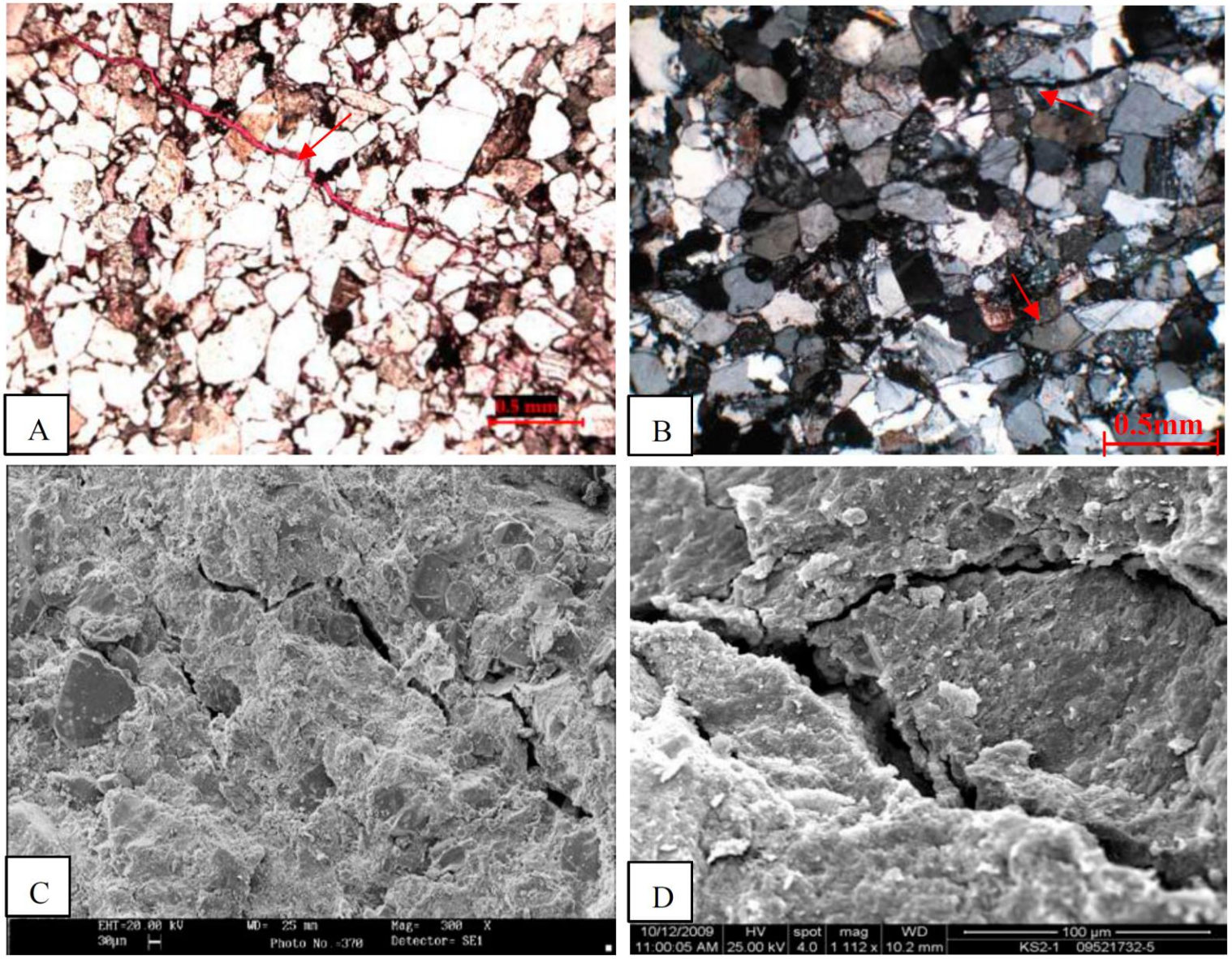

Figure 9. Traversing grain microfracture (arrow) in thin section from KS gas field. A= Traversing quartz grain microfracture, depth 6,930m (22,737ft). PPL. The red stained material is epoxy in the fracture pore space; B= Traversing quartz, feldspar grain and cement microfracture, depth 6,761m (22,183ft), XPL.C=Tectonic microfracture from DB gas field, depth 5,800m (19,030 ft). Aperture is 10 to 30 µm. SEM. D=Web tectonic microfractures, depth 6,604m (21,667.7ft). Aperture is 10 to 40 µm, SEM.

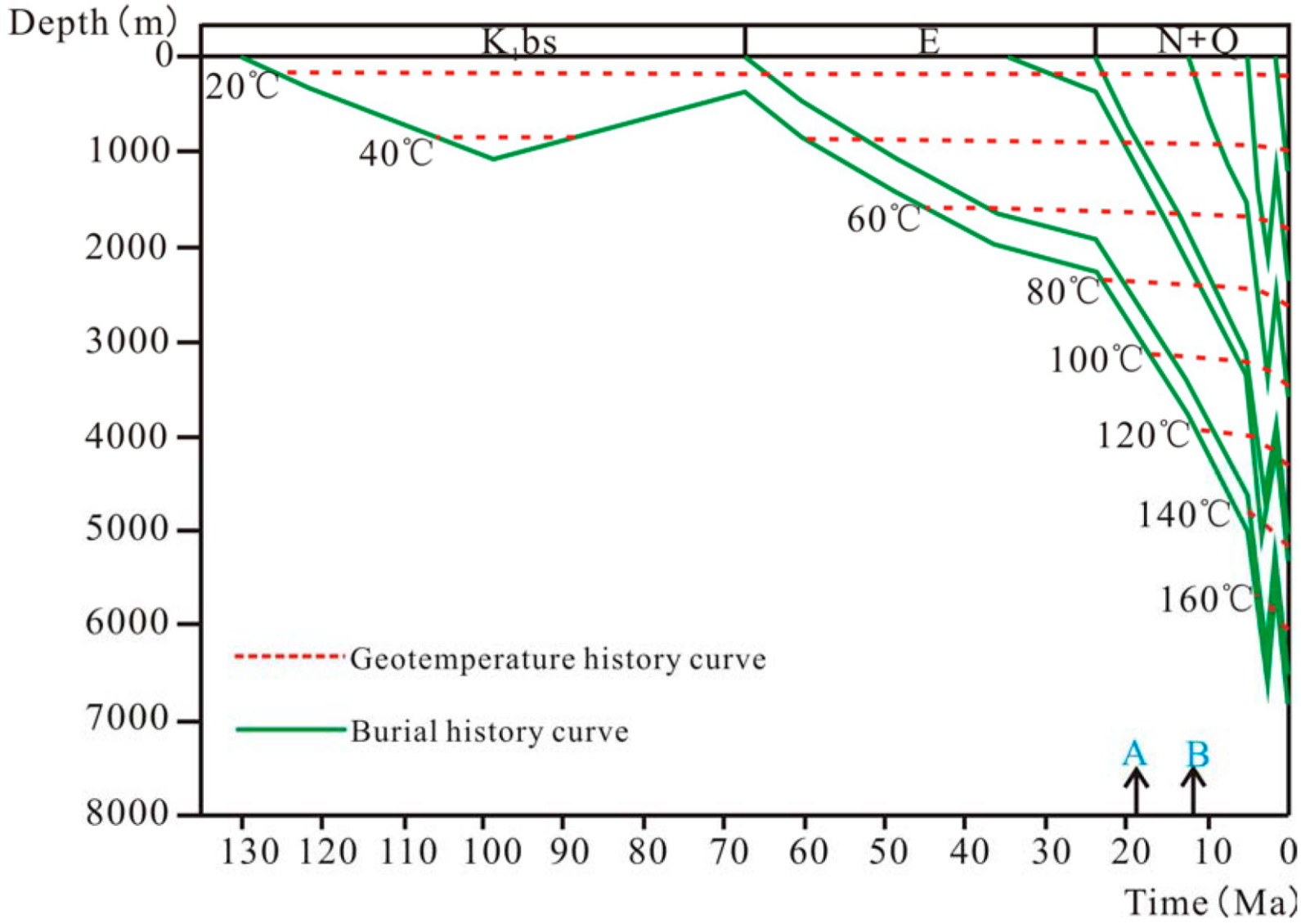

Figure 10. Burial history, geotemperature history, and fluid-inclusion homogenization temperature of anhydrite and calcite deposits in the tectonic microfractures in Lower Cretaceous Bashijiqike tight sandstones at the KS gas field (KS2 well).Burial history was deduced using compaction correction and regional denudation data. Geotemperature history was obtained by simulation using vitrinite reflectance data from Wang Feiyu et al. (2005). A=the first fracturing time from the oxygen stable isotope analysis of fracture-filling cements; B=the second fracturing time from fluid-inclusion homogenization temperatures more than 120°C.

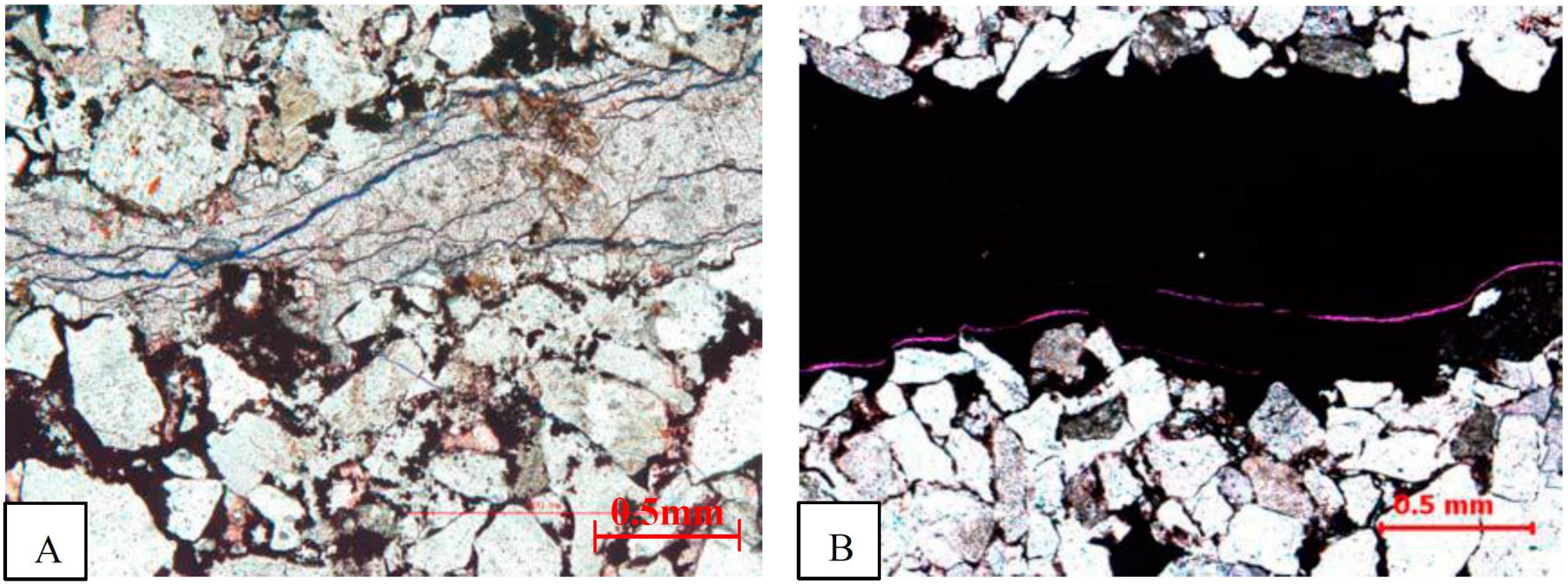

Figure 11. Diagenetic fracture along bedding plane and parallel to platy minerals in thin section. A= DB6 well, depth 6,858.37m, XPL. The blue stained material is epoxy; B=KS 202 well, depth 6,798.09m, the red stained material is epoxy, XPL.

Well number	Age	Location	depth range(m)	Reservoir type	Tectonic setting
DB202	K_1bs^{2-3}	DB gas field	5711-5956.5	gas	Foreland thrust belt
DB1	K_1bs^{3}	DB gas field	5550-5596	gas	Foreland thrust belt
DB101	K_1bs^{2-3}	DB gas field	5725-5914	gas	Foreland thrust belt
DB6	K^1bs^{2}	DB gas field	6847-6924	gas	Foreland thrust belt
DB103	K_1bs^{2-3}	DB gas field	5693.5-5946	gas	Foreland thrust belt
KS1	K_1bs^{1-2}	KS gas field	6904-7036	gas	Foreland thrust belt
KS2	K_1bs^{1-3}	KS gas field	6571.5-6780	gas	Foreland thrust belt
KS5	K_1bs^{1-3}	KS gas field	6703-6875	gas	Foreland thrust belt
KS201	K_1bs^{1-3}	KS gas field	6494-6793	gas	Foreland thrust belt
KS202	K_1bs^{1-3}	KS gas field	6699-6990	gas	Foreland thrust belt

Table 1. Units sampled for microfracture/macrofracture comparison.

Categories	Distribution	Length and Range	Aperture	Origin	application
Intragranular	Within coarse grain (quartz, feldspar)	Several tens of microns	<10 μm	diagenesis and/or tectonism	Local
Grain-Edge	Along coarse grain boundary	Several tens of microns	<10 μm	Diagenesis	Local
Transgranular	Traverse some grains and debris	From hundreds of microns to several centimeters	<40μm, mostly 10～20 μm	Tectonism and/or overpressure	Regional

Table 2. Microfracture categories and their interpreted origins.

Well number	Depth,m	Lithology	$\delta^{13}C_{PDB}$,‰	$\delta^{18}O_{PDB}$,‰	Equilibration Temperature(℃)
KS202	6765.32	fine sandstone	-3.777	-16.428	99.2
KS202	6799.18	fine sandstone	-2.760	-15.094	91.5
KS202	6799.31	fine sandstone	-2.887	-15.262	92.5
KS202	6799.58	fine sandstone	-3.475	-16.080	97.2
KS201	6513.35	fine sandstone	-3.493	-16.217	98.0

$ET = 0.04 \times (\delta^{13}O)^2 - 4.548 \times (\delta^{13}O) + 13.85$ *(PDB) (from Wuhan Geology Institute, 1979)*

Table 3. Oxygen and carbon isotopes of the calcite in fracture of Bashijiqike sandstone.